



The biologically active conformation of peptide 11
by Gerard Joseph Ostheimer

A thesis submitted in partial fulfillment of the requirements for the degree of Master of Science in
Chemistry

Montana State University

© Copyright by Gerard Joseph Ostheimer (1992)

Abstract:

The biological activities of biopolymers are a function of their three dimensional (3D) structure. Therefore, establishing the biologically active 3D structure of a biopolymer can provide unique insights into the mechanism by which that biopolymer functions. Peptide 11, a synthetic peptide, which is derived from the sequence of the basement membrane glycoprotein, laminin, disrupts metastatic invasion of tumor cells through the basement membrane matrix. Peptide 11 functions by interacting with the 67 kDa high affinity laminin receptor found on the surface of metastatic tumor cells (Iwamoto et al, 1987, Graf et al, 1987a, Graf et al, 1987b). In order to determine the structural properties responsible for its interaction with the 67 kDa high affinity laminin receptor, peptide 11 was studied by two-dimensional ^1H - ^1H nuclear magnetic resonance spectroscopy (NMR). NMR provides a powerful means of structure elucidation for biopolymers in solution (Wuthrich, 1986, Kessler et al., 1988, Wuthrich, 1989). Results of the application of NMR to determine the biologically active conformation of peptide 11 are presented in this thesis.

THE BIOLOGICALLY ACTIVE CONFORMATION OF PEPTIDE 11

by

Gerard Joseph Ostheimer

A thesis submitted in partial fulfillment
of the requirements for the degree

of

Master of Science

in

Chemistry

Montana State University
Bozeman, MT

December 1992

11378
Ds 76

APPROVAL

of a thesis submitted by

Gerard Joseph Ostheimer

This thesis has been read by each member of the thesis committee and has been found to be satisfactory regarding content, English usage, format, citations, bibliographic style, and consistency, and is ready for submission to the College of Graduate Studies.

2/3/93
Date

Edward A. [Signature]
Chairperson, Graduate Committee

Approved for the Major Department

2/3/93
Date

John R. [Signature]
Head, Major Department

Approved for the College of Graduate Studies

2/3/93
Date

R. L. [Signature]
Graduate Dean

STATEMENT OF PERMISSION TO USE

In presenting this thesis in partial fulfillment of the requirements for a master of science degree from Montana State University, I agree that the Library shall make it available to borrowers under the rules of the Library. Brief quotations from this thesis are allowable without special permission, provided that accurate acknowledgement of source is made.

Permission for extensive quotation from or reproduction of this thesis may be granted by my major professor, or in his absence, by the Dean of Libraries when, in the opinion of either, the proposed use of the material is for scholarly purposes. Any copying or use of the material in this thesis for financial gain shall not be allowed without my written permission.

Signature



Date

12/6/92

TABLE OF CONTENTS

| | Page |
|---|------|
| TABLE OF CONTENTS | iv |
| LIST OF TABLES | vi |
| LIST OF FIGURES | vii |
| ABSTRACT | ix |
| 1. INTRODUCTION | 1 |
| The Use of NMR to Study Peptide Conformation | 1 |
| NOESY of Short, Linear Peptides Free in Solution | 2 |
| Transferred Nuclear Overhauser Effect Spectroscopy | 3 |
| The Biological Activity of Peptide 11 | 8 |
| Prior Computational Studies of Peptide 11 Conformation | 9 |
| The Use of Amino Acid Substitution to Determine the Biologically Active Conformation of Peptide 11 | 10 |
| 2. MATERIALS AND METHODS | 15 |
| Peptide Synthesis | 15 |
| Isolation of the 67 kDa High-Affinity Laminin Receptor | 15 |
| Composition of Solution State NMR Samples | 19 |
| NMR Spectroscopy Experimental Parameters | 20 |
| Processing of NMR Data | 22 |
| Determination of Average Inter-Proton Distances | 23 |
| Incorporation of Pseudo-atoms | 25 |
| Molecular Dynamics | 26 |
| 3. PEPTIDE 11 IN AQUEOUS SOLUTION | 29 |
| Chemical Shift Behavior | 39 |

TABLE OF CONTENTS - continued

| | |
|---|---------|
| Two Spin Systems are Assignable to the CDPG Regions of the Peptides Free in Solution at pH ~5 | 42 |
| NOESY of the Peptides Free in Aqueous Solution | 44 |
| Molecular Dynamics | 54 |
| Unconstrained Molecular Dynamics | 71 |
| ϕ, ψ Plots of Free Peptide Conformations | 71 |
| Observation of a DPGY Turn | 81 |
| TRNOESY Experiments are Required | 82 |
| 4. THE RECEPTOR BOUND CONFORMATION OF PEPTIDE 11 | 83 |
| Evidence for Binding of the Peptides to the Receptor | 83 |
| The Chemical Shift Values of Cys ₁ Protons in the Presence of Receptor Differ From Their Free in Solution Values | 84 |
| Peptide Cross Relaxation Rates Are Faster in the Presence of Receptor | 85 |
| Relative NOE and TRNOE Intensities Differed Considerably | 102 |
| J ³ Coupled Protons Exhibited Zero Quantum Coherence | 103 |
| Conformations of the Peptides in the Presence of Receptor | 107 |
| DPGY of All Three Peptides Forms a Type II β Turn in the Receptor Bound Conformation | 107 |
| YIGSR of Peptide 11 Forms a Bend in the Receptor Bound Conformation | 108 |
| YIASR of the D-analog Forms a Bend | 109 |
| YIASR of the L-analog is in an Extended Conformation | 109 |
| Generation of Candidate Receptor Bound Conformations by Molecular Dynamics | 110 |
| 5. DISCUSSION | 118 |
| The Activity of the D-analog and Peptide 11 are Equal | 118 |
| YIXSR Conformations of Peptide 11 and the D-analog With Good NOE Agreement Match the Predictions of Brandt-Rauf <i>et al.</i> | 119 |
| YIGSR-NH ₂ and YI(dA)SR-NH ₂ are Active, YI(IA)SR-NH ₂ is Inactive | 120 |
| The L-analog, CDPGYI(IA)SR-NH ₂ , Possesses Residual Activity | 121 |
| Cys ₁ is Required for the CDPG Region of Peptide 11 to Effectively Bind to the Receptor | 121 |
| Arg ₉ Stabilizes the YIXSR Bend | 122 |
| IGSR is Inactive | 125 |
| How the Receptor Binds Peptide 11 | 125 |
| Conclusion | 125 |
| REFERENCES | 127 |

LIST OF TABLES

| Table | Page |
|---|------|
| 1. Longitudinal Relaxation Times (T_1) of the Different Species of Protons Found in Peptide 11 | 21 |
| 2. The Chemical Shift (ppm) of the Protons in Peptide 11 Compared to Random Coil Values* | 36 |
| 3. The Chemical Shift (ppm) of the Protons in the D-analog Compared to Random Coil Values* | 37 |
| 4. The Chemical Shift in ppm of the Protons in the L-analog Compared to Random Coil Values* | 38 |
| 5. The Chemical Shifts of the Two Spin Systems of Cys ₁ Found in the Free Peptide at pH ~5 | 43 |
| 6. Cys ₁ Chemical Shifts | 84 |
| 7. Peptide 11 Free in Solution NOE Intensities as a Function of Mixing Time (t_m) | 87 |
| 8. D-analog Free in Solution NOE Intensities as a Function of Mixing Time (t_m) | 89 |
| 9. L-analog Free in Solution NOE Intensities as a Function of Mixing Time (t_m) | 91 |
| 10. Peptide 11 TRNOE Intensities as a Function of Mixing Time (t_m) ... | 93 |
| 11. D-analog TRNOE Intensities as a Function of Mixing Time (t_m) | 95 |
| 12. L-analog TRNOE Intensities as a Function of Mixing Time (t_m) | 97 |
| 13. The Effect of Receptor Binding on Peptide 11 Inter-residue NOE Intensity | 104 |
| 14. The Effect of Receptor Binding on D-analog Inter-residue NOE Intensity | 105 |
| 15. The Effect of Receptor Binding on L-analog Inter-residue NOE Intensity | 106 |
| 16. Predictions of YIXSR Conformation | 119 |

LIST OF FIGURES

| Figure | Page |
|---|------|
| 1. NOE Intensity Dependence on Correlation Time (t_c) | 4 |
| 2. Dose Dependent (mM) Inhibition (%) of Metastatic Cell Migration <i>in vitro</i> by Peptide 11, the D-analog, and the L-analog | 12 |
| 3. SDS-Page of the Material Extracted From EHS Tumor | 18 |
| 4. J+R NOESY Pulse Sequence and Phase Cycling | 22 |
| 5. Peptide 11 Sequential Backbone Connectivity as Shown by ROESY .. | 30 |
| 6. D-analog Sequential Backbone Connectivity as Shown by ROESY | 31 |
| 7. L-analog Sequential Backbone Connectivity as Shown by ROESY | 32 |
| 8. The Proton Assignments of Peptide 11 as Shown by TOCSY | 33 |
| 9. The Proton Assignments of the D-analog as Shown by TOCSY | 34 |
| 10. The Proton Assignments of the L-analog as Shown by TOCSY | 35 |
| 11. Peptide 11 Sequential Backbone Connectivity as Found in NOESY .. | 47 |
| 12. D-analog Sequential Backbone Connectivity as Found in NOESY | 48 |
| 13. L-analog Sequential Backbone Connectivity as Found in NOESY | 49 |
| 14. The NH_i-NH_{i+1} Connectivity of Peptide 11 | 50 |
| 15. The NH_i-NH_{i+1} Connectivity of the D-analog | 51 |
| 16. The NH_i-NH_{i+1} Connectivity of the L-analog | 52 |
| 17. The $NH_i-\beta H_i$ and βH_i-NH_{i+1} Connectivity of Peptide 11 | 55 |
| 18. The $NH_i-\beta H_i$ and βH_i-NH_{i+1} Connectivity of the D-analog | 56 |
| 19. The $NH_i-\beta H_i$ and βH_i-NH_{i+1} Connectivity of the L-analog | 57 |
| 20. Free Peptide 11 NOE Deviation | 58 |
| 21. Free D-analog NOE Deviation | 59 |
| 22. Free L-analog NOE Deviation | 60 |
| 23. Free Peptide 11 Energy | 61 |
| 24. Free D-analog Energy | 62 |
| 25. Free L-analog Energy | 63 |
| 26. Peptide 11 Free in Solution | 65 |
| 27. Peptide 11 Free in Solution | 66 |
| 28. The D-analog Free in Solution | 67 |
| 29. The D-analog Free in Solution | 68 |
| 30. The L-analog Free in Solution | 69 |
| 31. The L-analog Free in Solution | 70 |
| 32. Free Peptide 11 Energy During Unconstrained Molecular Dynamics | 72 |
| 33. NOE Deviation During Unconstrained Molecular Dynamics of Peptide 11 | 73 |

LIST OF FIGURES - continued

| Figure | Page |
|--|------|
| 34. Conformation of Peptide 11 Generated by Unconstrained Molecular Dynamics | 74 |
| 35. Conformation of Peptide 11 Generated by Unconstrained Molecular Dynamics | 75 |
| 36. ϕ, ψ Plots of Free Peptide 11 | 77 |
| 37. ϕ, ψ Plots of the D-analog Free in Solution | 78 |
| 38. ϕ, ψ Plots of the L-analog Free in Solution | 79 |
| 39. ϕ, ψ Plots of Free Peptide 11 Unconstrained | 80 |
| 40. Peptide 11 Ile ₆ NH-Gly ₇ NH NOE and TRNOE Intensity as a Function of Mixing Time (t_m) | 99 |
| 41. D-analog Ala ₇ α H-Ser ₈ NH NOE and TRNOE Intensity as a Function of Mixing Time (t_m) | 100 |
| 42. L-analog Ser ₈ α NH-Arg ₉ NH NOE and TRNOE Intensity as a Function of Mixing Time (t_m) | 101 |
| 43. Peptide 11 Bound to the Receptor | 111 |
| 44. Peptide 11 Bound to the Receptor | 112 |
| 45. The D-analog Bound to the Receptor | 113 |
| 46. The D-analog Bound to the Receptor | 114 |
| 47. The L-analog Bound to the Receptor | 115 |
| 48. The L-analog Bound to the Receptor | 116 |
| 49. SDPGYIGSR-NH ₂ is Inactive | 123 |

ABSTRACT

The biological activities of biopolymers are a function of their three dimensional (3D) structure. Therefore, establishing the biologically active 3D structure of a biopolymer can provide unique insights into the mechanism by which that biopolymer functions. Peptide 11, a synthetic peptide, which is derived from the sequence of the basement membrane glycoprotein, laminin, disrupts metastatic invasion of tumor cells through the basement membrane matrix. Peptide 11 functions by interacting with the 67 kDa high affinity laminin receptor found on the surface of metastatic tumor cells (Iwamoto *et al.*, 1987, Graf *et al.*, 1987a, Graf *et al.*, 1987b). In order to determine the structural properties responsible for its interaction with the 67 kDa high affinity laminin receptor, peptide 11 was studied by two-dimensional ^1H - ^1H nuclear magnetic resonance spectroscopy (NMR). NMR provides a powerful means of structure elucidation for biopolymers in solution (Wüthrich, 1986, Kessler *et al.*, 1988, Wüthrich, 1989). Results of the application of NMR to determine the biologically active conformation of peptide 11 are presented in this thesis.

CHAPTER 1

INTRODUCTION

The Use of NMR to Study Peptide Conformation

The use of NMR to study the conformation of short, linear peptides, such as peptide 11, when free in aqueous solution, has several inherent difficulties (Wright *et al.*, 1988). The energy barriers separating low energy backbone conformations of short, linear peptides have been estimated to be on the order of 1-3 kilocalories per mole (Zimmerman *et al.*, 1977). Such low energy barriers between conformations permit short peptides to sample conformation space on the millisecond or shorter timescale (reviewed by Rose *et al.*, 1985). As short peptides are constantly in the process of sampling conformation space, only a fraction of the molecules possess compact conformations at any one time.

The timescale of NMR experiments is on the order of milliseconds; therefore, molecular structures must exist for greater than milliseconds in order to be directly studied by solution state NMR. Short peptides explore conformation space rapidly on the NMR timescale. As a result of their rapid exploration of conformation space, the structural parameters of short peptides measured by NMR are an average of all different compact peptide conformations as well as the conformations of "unfolded" peptides in the process of exploring conformation space. Properties of interest to

biopolymer structure elucidation that are detectable by NMR include inter-proton distances, bond angles, chemical shifts, and the presence of hydrogen bonding. These parameters are all subject to the aforementioned time averaging.

NOESY of Short, Linear Peptides Free in Solution

Inter-proton distances can be measured by monitoring the through space dipolar magnetic cross-relaxation between the protons of interest (Jeener *et al.*, 1979, Macura and Ernst, 1980, Ernst *et al.*, 1987). This through space dipolar coupling is referred to as the nuclear Overhauser effect (NOE). NOE intensity is a function of the average distance between the two nuclei (r_{ij}), the correlation time (τ_c) of the molecule, and the mixing time (τ_m).

$$\text{NOE} \propto \langle r_{ij}^{-6} \rangle \cdot f(\tau_c) \cdot g(\tau_m)$$

Because the nuclear Overhauser effect diminishes rapidly with distance ($\propto \langle r_{ij}^{-6} \rangle$), the maximum inter-proton distance measureable in solution is approximately 5 Å.

The NOEs of short peptides free in solution are weighted towards compact conformations. Unless $r_{ij} < 3.5$ Å the NOE interaction will typically not be sufficiently strong to observe even if a long mixing time is employed (Dyson *et al.*, 1988a,b). This reduction in the range of NOE detection from 5.0 Å to 3.5 Å results from the NOE dependence on the rotational correlation time (τ_c) of the inter-proton vectors of the molecule under study. τ_c is a function of the viscosity of the solvent (η), the radius of the molecule (a) and the temperature of the solvent (T). For spherical molecules in solution:

$$\tau_c = 4\pi a^3 / 3kT$$

(k = Boltzmann's constant). When studied with high field ($300 \text{ MHz} \geq \omega_0 \geq 600 \text{ MHz}$) NMR spectrometers, small molecules, with short τ_c ($\sim 10^{-11}$ sec.) exhibit strong positive NOEs, and large molecules, with long τ_c ($\sim 10^{-8}$ sec.) exhibit strong negative NOEs (Fig. 1). Short peptides, in non-viscous solvents, possess intermediate correlation times which result in values of $\omega_0 \tau_c \leq 1$ (ω_0 = experimental proton resonance frequency), for which NOE intensity is a minimum (Ernst *et al.*, 1987).

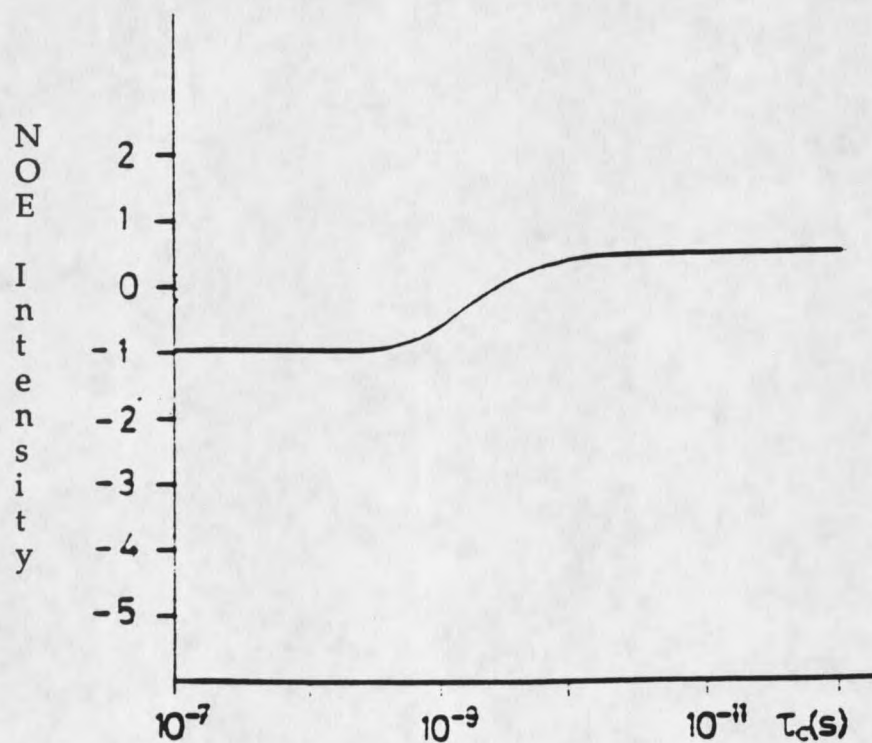
The range of measureable r_{ij} in short peptides free in solution is ≤ 3.5 Å. In an extended peptide, both non-sequential inter-residue distances and the sequential inter-residue distances $d_{\text{NN}}(i,i+1)$ and $d_{\beta\text{N}}(i,i+1)$, which range from 1.5 Å to 4.5 Å, will be greater than 3.5 Å. Therefore, detection of inter-residue NOEs indicates the existence of compact peptide conformations in solution. However, of the many low energy compact conformations accessible to a peptide free in aqueous solution (Zimmerman *et al.*, 1977), only a few, if any, very closely related conformations are likely to be responsible for its biological activity. Unfortunately, it is impossible to quantitate by solution NMR what fraction of the free peptide conformer population is biologically active. Therefore, it is not possible to specify the biologically active conformation of a short, linear peptide solely by NMR spectroscopy of the peptide free in solution.

Transferred Nuclear Overhauser Effect Spectroscopy

A short flexible peptide ligand need only possess its biologically active

Figure 1. NOE Intensity Dependence on Correlation Time (τ_c).

When studied at high magnetic fields, inter-proton NOE intensity is large and negative for $\tau_c < \sim 10^{-9}$ s and large and positive for $\tau_c > \sim 10^{-11}$ s. If τ_c is in between this range ($\omega_0\tau_c \approx 1$), then inter-proton NOE intensity is at a minimum. The τ_c of peptide 11 is in the range for which NOE intensity is a minimum.



conformation when it is bound to its receptor. Evidence for the structure of a peptide ligand when bound to its receptor can be determined by using the 1D time-dependent intramolecular transferred Nuclear Overhauser Effect (TRNOE) (Balaram *et al.*, 1972a, Balaram *et al.*, 1972b, Clore and Gronenborn, 1982, Clore and Gronenborn, 1983) or the 2D intramolecular TRansferred Nuclear Overhauser Effect Spectroscopy (TRNOESY, Clore and Gronenborn, 1986, Campbell and Sykes, 1991a, Campbell and Sykes, 1991b). For large molecules, such as cell surface receptors like the 67 kDa high-affinity laminin receptor, $\tau_c > 10^{-8}$ seconds and $\omega_0\tau_c \gg 1$. The long correlation time of large molecules results in extremely efficient magnetic cross-relaxation between protons but very broad linewidths. The efficient magnetic cross-relaxation of small molecules when bound to the large molecule results in the small molecule exhibiting strong negative NOEs (Fig. 1).

When a ligand binds to its receptor its correlation time slows from its value free in solution to a value close to that of the receptor. The rate of cross-relaxation between the protons i and j (W_{ij}) of the peptide increases as a result of receptor binding. Receptor bound magnetic cross-relaxation rates (W_{ijB}) are far greater than the magnetic cross-relaxation rates of the peptide free in solution (W_{ijF}). Therefore, NOE intensities of receptor bound peptides build much faster than NOE intensities of peptides free in solution. Unfortunately, it is not possible to directly observe the peptide by solution state NMR when it is bound to a large receptor protein. The long τ_c of molecules which are 50 kilo-Daltons (kDa) or larger exhibit line widths that are too broad to be observed by NMR. However, if the peptide ligand were to dissociate from its receptor, then its τ_c would decrease to its shorter free in

solution value, and the peptide would again be NMR observable.

The magnetic cross-relaxation between protons of a short peptide is significantly slower when it is free in solution. Therefore, the distribution of magnetization that results from rapid nuclear Overhauser cross-relaxation in the bound state, and the structural information the magnetization contains, is lost more slowly in the free peptide. The receptor bound magnetization, and the structural information contained therein, can be measured by NOESY. Through chemical exchange, the information concerning the bound state has been "transferred" to the free state where it can be measured. For this transferral to be effective, the peptide ligand must exchange rapidly between the free and the bound state relative to the rate of magnetic longitudinal relaxation (T_1 relaxation) of the free peptide.

As cross-relaxation rates are relatively rapid for large molecules, unwanted spin diffusion can occur between the protons of the peptide ligand, while it is receptor bound. Spin diffusion alters NOE intensities in complex ways, and consequently disrupts attempts to use NOE intensity to calculate r_{ij} . Recently, Campbell and Sykes have evaluated the effects of mixing time (τ_m), receptor bound correlation time (τ_{cB}), and fraction of bound peptide (p_B) on TRNOESY intensity and on the inter-proton distances calculated from these intensities (Campbell and Sykes, 1991a). They found spin diffusion to occur quite rapidly on the NMR timescale. The effects of τ_m , τ_{cB} , and p_B are additive, so each can be considered independently. Spin diffusion is maximized at long τ_m , long τ_c , and high p_B . In order to achieve a decent signal-to-noise ratio, Campbell and Sykes suggest that "it is best to use very low p_B values but work at a reasonable τ_m " (ie. ≤ 200 ms). In the discussion of

their results they provide the following example, "for a protein of $M_r \approx 80,000$ Da one need only bind 5% of the peptide to achieve both a huge enhancement in the size of the TRNOE and a linear buildup of magnetization for reasonable mixing times."

If the p_B is relatively small (ie. $< 5\%$), then interference from NMR detection of the free ligand might be anticipated. For small p_B both the chemical shift ($\delta_{\text{obs}} = p_F\delta_F + p_B\delta_B$) and the linewidth ($\Delta\nu_{\text{obs}} = p_F\Delta\nu_F + p_B\Delta\nu_B$) will be dominated by the free peptide (Campbell and Sykes, 1991b). However, due to the difference in cross-relaxation rates mentioned earlier ($W_{ijB} \gg W_{ijF}$), the observed NOEs will be TRNOE dominated, $\text{NOE}(\tau_m) \approx -[p_F W_{ijF} + p_B W_{ijB}]\tau_m \approx -[p_B W_{ijB}]\tau_m$, at "reasonable" τ_m (Campbell and Sykes, 1991b). Interestingly, for a p_B as low as 0.5% the distances derived from TRNOE cross peak intensity correspond quite well to the inter-proton distances of the bound peptide (Campbell and Sykes, 1991a). As opposed to NOEs measured from short peptides free in solution, TRNOESY distance measurements relate directly to the bound, biologically active conformation, and can therefore be used to provide information on the biologically active conformation of a short peptide. TRNOESY has been used to gain insights concerning the interactions between fibrinogen derived peptides and thrombin (Ni *et al.*, 1989a-1989c), the interactions of troponin I and troponin C (Campbell and Sykes, 1991a), the different conformations of peptides when bound to the chaperones DnaK and GroEL (Landry *et al.*, 1992) and in other systems, as well.

The Biological Activity of Peptide 11

Laminin is the primary glycoprotein of basement membranes (Timpl *et al.*, 1979; Chung *et al.*, 1979). It is composed of three chains: A (440,000 kDa), B1 (225,000 kDa), and B2 (205,000 kDa), which combine to form a cruciform shaped structure (Engel *et al.*, 1981). Various domains of laminin have been shown to promote attachment to basement membranes, migration through basement membranes, and growth and differentiation of certain cell types (reviewed by Beck *et al.*, 1990, Goodman, 1992, and Starkey, 1990). Metastatic ability has been shown to correlate with the expression of 67 kDa high-affinity laminin receptor (Terranova *et al.*, 1983, Wewer *et al.*, 1986). High concentrations of this cell surface receptor improve the ability of these cells to attach to, and to subsequently migrate through, basement membranes. Metastatic cells employing the 67 kDa high-affinity laminin receptor to adhere to the basement membrane interact with the laminin B1 chain near its intersection with the other two chains (Graf *et al.*, 1987a). The 67 kDa high-affinity laminin receptor is not the only means by which metastatic cells interact with laminin. Other laminin receptors include the $\alpha 6\beta 1$ (Ramos *et al.*, 1991) and $\alpha 7\beta 1$ (Kramer *et al.*, 1991) integrins.

Peptide 11, CDPGYIGSR, which corresponds to residues 924-933 of the laminin B1 chain has been shown to inhibit the attachment of tumor cells to laminin (Graf *et al.*, 1987a), inhibit migration of tumor cells through a basement membrane matrix Matrigel © (Ostheimer *et al.*, 1992), which is a reconstitution of a urea extraction of basement membranes (Kleinman *et al.*, 1986), and decrease tumor lung colony formation *in vivo* (Iwamoto *et al.*, 1987, Ostheimer *et al.*, 1992). The minimum sequence necessary for biological

activity is YIGSR. Either deletion of tyrosine or substitution of lysine or glutamine for arginine is sufficient to destroy YIGSR activity (Graf *et al.*, 1987b). The amide form of peptide 11, CDPGYIGSR-NH₂, is more active (Iwamoto, *et al.*, 1987), and hereafter, the name peptide 11 will refer to the amide form, which was the form of the peptide used in this work. The biological effects of Peptide 11 are believed to result from binding to the 67 kDa high affinity laminin receptor found on the metastatic cells, blocking the normal laminin binding site, and thereby reducing the capacity of the metastatic cells to adhere to basement membranes via laminin (Iwamoto *et al.*, 1987, Ostheimer *et al.*, 1992).

Prior Computational Studies of Peptide 11 Conformation

The YIGSR region of peptide 11 has been previously investigated by molecular dynamics (MD) (Brandt-Rauf *et al.*, 1989, McKelvey *et al.*, 1991). However, as neither of the two previous studies incorporated experimentally derived structural information into their calculations, the structures they propose for YIGSR are strictly predictions.

Brandt-Rauf *et al.* calculated the lowest energy conformation of N-Acetyl-YIGSR-NHCH₃ using the modelling software, ECEPP (Empirical Conformational Energy for Polypeptides and Proteins, Scheraga, 1984). They predicted that the backbone conformation of the YIGSR sequence would correspond to regions C-D-D*-D-D of a Zimmerman ϕ, ψ plot (Zimmerman *et al.*, 1977). A Zimmerman ϕ, ψ plot is a Ramachandran plot, to which regions corresponding to conformational energy minima have been assigned a single letter code. Unstarred letters indicate ϕ to be in the range, $-180^\circ \leq \phi \leq 0^\circ$, and

starred letters indicate ϕ to be in the range, $0^\circ \leq \phi \leq 180^\circ$. C-D-D*-D-D consists of a bend about the glycine residue held in place by a hydrogen bond between the NH_2 of the arginine side chain and the backbone C=O of tyrosine.

McKelvey *et al.* calculated the lowest energy conformation N-Acetyl-YIGSR-NHCH₃ using the molecular mechanics program CHARMM (Chemistry at HARvard Macromolecular Mechanics, Brooks *et al.*, 1983).

McKelvey *et al.* predicted that for dielectric constants ranging from 1 to 10 that the conformation of the YIGSR sequence would correspond to Zimmerman regions CA-A-A-F-E/C. CA being a previously undefined region of the Zimmerman plot found between regions C and A. CA-A-A-F-E/C corresponds to a partial helical conformation, which McKelvey *et al.* found to be stabilized by hydrogen bonds between the NH_2 of the arginine side chain and the C=O of tyrosine, isoleucine, and glycine. Although Brandt-Rauf *et al.* and McKelvey *et al.* both predicted YIGSR to adopt a bent conformation, the type of bend differed greatly between the predictions of the two groups.

The Use of Amino Acid Substitution to Determine the Biologically Active Conformation of Peptide 11

The prediction of a turn about the glycine of YIGSR is not unexpected. Glycine lacks a side chain and is therefore achiral. Because glycine does not possess a side chain, it is free to explore all four quadrants of ϕ, ψ space. In contrast, the side chains of l-stereoisomeric amino acids sterically forbid them from adopting conformations corresponding to quadrant IV of a ϕ, ψ plot. Consequently, glycine frequently plays the role of a hinge, allowing protein backbones to make tight turns and bends not allowed by other amino acids.

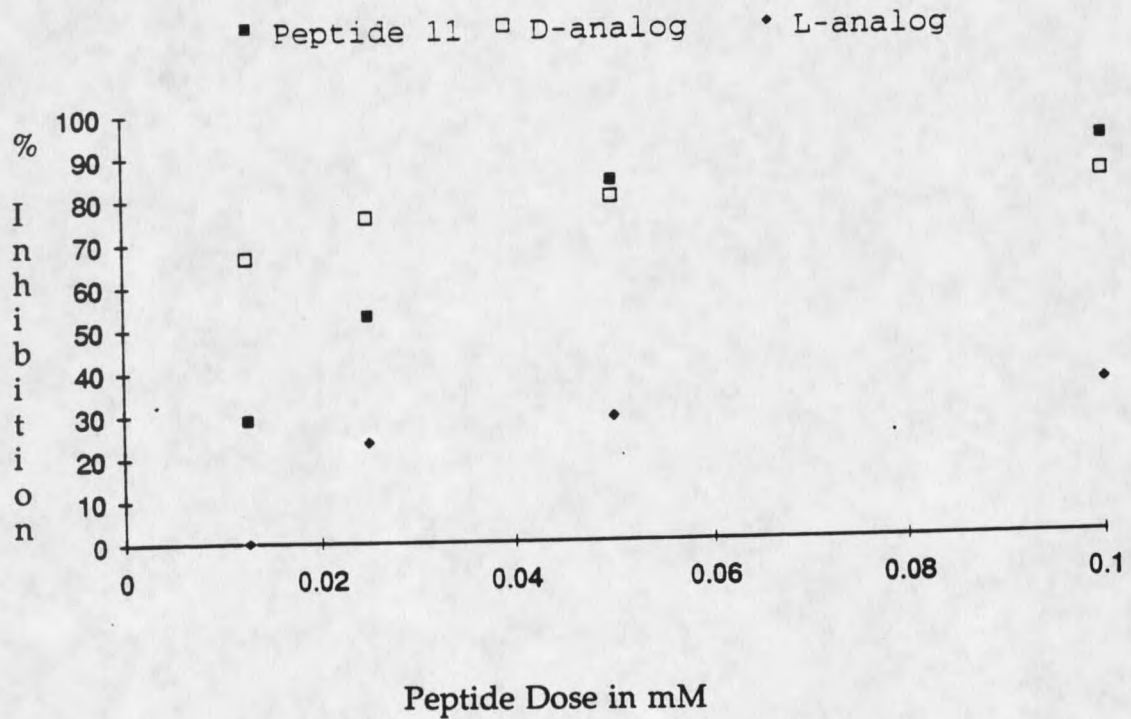
The predictions of a glycine centered YIGSR bend by Brandt-Rauf *et al.*

and McKelvey *et al.* can be tested by substituting chiral amino acids for the achiral glycine. Substitution of d-alanine and l-alanine for Gly₇ would prevent the backbone of peptide 11 from adopting conformations at its seventh residue corresponding to ϕ, ψ quadrants III and IV, respectively. The d-alanine₇ analog, CDPGYI(dA)SR-NH₂ (d-analog), was found to be as capable as the native peptide 11 of inhibiting cell migration *in vitro* at high concentrations (0.10 mM) and to be more effective than peptide 11 at lower concentrations (0.0125 mM) (Fig. 2). The increased activity of the d-analog at low peptide concentrations is thought to be at least partly due to the fact that d-Ala₇ is more resistant to protease activity than the native Gly₇. The presence of proteases was expected as intact cells are present in the *in vitro* assay employed to determine peptide activity.

In contrast, the l-alanine₇ analog, CDPGYI(lA)SR-NH₂ (l-analog), was found to be considerably less active than peptide 11 and the d-analog at both low and high concentrations (Fig. 2). The different activities of the d and l-analogs suggests that the biological activity of peptide 11 results in part from the conformation of the YIGSR region of the molecule. To test this hypothesis 2D ¹H-¹H NMR spectroscopy was employed to measure structural parameters of peptide 11, the d-analog, and the l-analog when free in solution and when bound to the 67 kDa high affinity laminin receptor. The structural information derived from NMR was incorporated into molecular dynamics simulations of the peptides in order to generate candidate structures for the biologically active conformation of peptide 11.

As per the earlier discussion of short, linear peptides free in aqueous solution, it is typically not possible to directly determine the biologically

Figure 2. Dose Dependent (mM) Inhibition(%) of Metastatic Cell Migration *in vitro* by Peptide 11, the D-analog, and the L-analog.



active conformation of a short peptide when it is free in solution. However, in this system, it was believed that a comparison of the free in solution candidate conformations of peptide 11 with the free in solution candidate conformations of the equally active and less active analogs might suggest conformational properties responsible for the biological activity of peptide 11.

NMR spectroscopy indicated that peptide 11 and the d-analog behaved similarly, and simultaneously quite differently from the l-analog when free in solution. When the NMR derived distance constraints were incorporated into molecular dynamics simulations quite similar conformations for peptide 11 and the d-analog were generated. The conformations generated for the l-analog were very different from those preferred by peptide 11 and the d-analog. These conformations, and the data used to derive them, will be described and discussed below.

TRNOESY experiments successfully indicated the receptor bound conformation of peptide 11 and the d and l-analogs. Based on TRNOESY cross peak patterns, it was possible to identify the secondary structures possessed by the bound peptides. In order to visualize the peptide conformations, TRNOE intensities were converted into inter-proton distances, which were then employed to restrain molecular dynamics simulations. The peptide conformations generated by the molecular dynamics are presented, and their biological relevance are discussed below.

Other groups of researchers are employing NMR spectroscopy to elucidate the structure/function relationships of peptides derived from proteins involved in cell adhesion. Data exists concerning peptides containing the RGD (arginine-glycine-aspartic acid) sequence (Reed *et al.*, 1988,

Bogusky *et al.*, 1992) and non-RGD cell adhesion promoting peptides from collagen, fibrinogen, and laminin (Mayo *et al.*, 1991, Mayo *et al.*, 1990, Burke *et al.*, 1991).

CHAPTER 2

MATERIALS AND METHODS

Peptide Synthesis

Peptide 11, the d-alanine₇ analog (d-analog), and the l-alanine₇ analog (l-analog) were synthesized, purified, and analyzed by Craig Johnson at the MSU Peptide Synthesis Facility. Peptides were synthesized on a Milligen 9050 Peptide Synthesizer using standard Fmoc chemistry with Bop/Hobt activation. DMF, DCM, acetic anhydride, and piperidine were of spectrophotometric grade as supplied by Aldrich Chemical Co. Peptides were purified by HPLC using a Vydac C18 reverse phase preparatory column, and analyzed on a Vydac C18 reverse phase analytical column. Peptide purity was estimated to be greater than or equal to 90%. Molecular weights were checked by probe FAB mass spectrometry, which was performed by Joe Sears at the MSU Mass Spectrometry Facility.

Isolation of the 67 kDa high-affinity laminin receptor

All samples of the 67 kDa high-affinity laminin receptor were prepared by Terry Landowski and Jean Starkey. The 67 kDa high-affinity laminin receptor was isolated from EHS mouse tumor using a modified laminin extraction process (Timpl *et al.*, 1979). EHS tumor was propagated by subcutaneous transplant in C57BL/6 mice. Tumors were harvested after having grown to be approximately 1.5 to 2.0 cm in diameter. Harvested

material was washed extensively in 4° C Tyrode's calcium and magnesium free saline and stored at -20° C until used.

Tumor thawed at 4° C was covered with an equal volume of ice cold buffer containing 3.4 M NaCl, 0.05 M Tris-HCl, pH 7.4, 0.01 M ethylenediaminetetraacetic acid (EDTA) plus the protease inhibitors Benzamidine, N-ethylmaleamide (NEM), and phenylmethanesulfonyl flouride (PMSF). The preparation was homogenized on ice for approximately 20 minutes with a Polytron homogenizer, centrifuged for 10 minutes at 12,000 x g, and the supernatant discarded. Homogenization was repeated 2-3 times until the material became a thick slurry, which was then suspended in 10 volumes (v/v) of 0.5 M NaCl, 0.05 M Tris, pH 7.4, and the same protease inhibitors. Basement membrane components were extracted by mechanical stirring overnight at 4° C, followed by centrifugation for 20 minutes at 10,000 x g. The supernatant was made 1.7 M in NaCl and stirred on ice for 2 hours to precipitate type IV collagen, which was then removed by 30 minutes of centrifugation at 10,000 x g. The supernatant was dialyzed against a solution of 2 M urea, 0.05 M Tris-HCl, pH 8.6. Silver-stained SDS-Page electrophoresis of the urea treated material showed it to consist predominantly of laminin and a band characteristic of the 67 kDa high-affinity laminin receptor. Minor additional bands were present at 90, 55, and 40 kDa (data not shown).

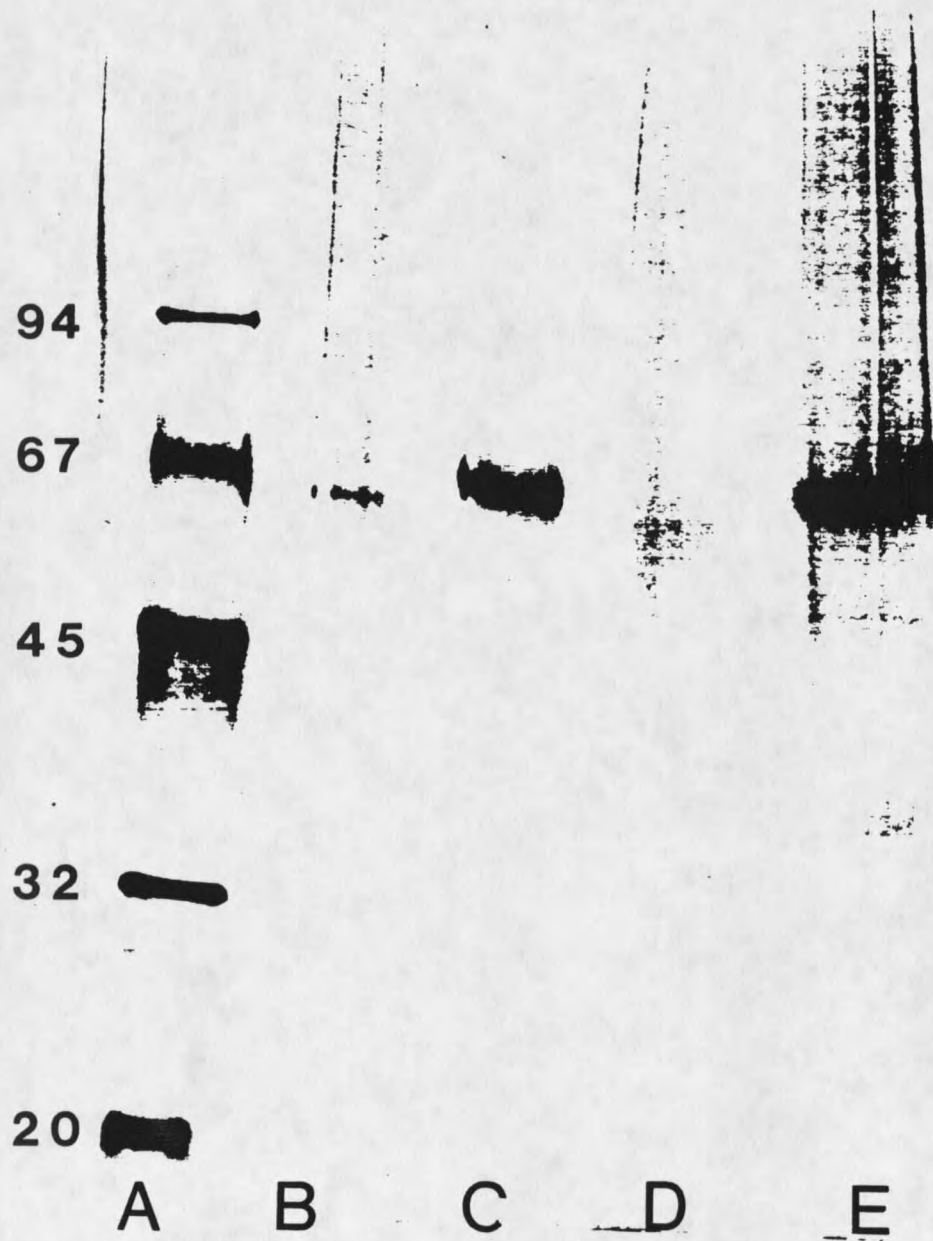
Laminin receptor was then extracted from the urea treated material by the method of Folch et al. (1957). The material extracted from EHS tumor was mixed with 20 volumes of chloroform:methanol (2:1, v/v) and mechanically stirred at room temperature for one hour, after which time it was allowed to

partition into aqueous and organic phases. The organic phase, which contained the laminin receptor, was collected through the bottom of a separatory funnel. Great care was taken to exclude the aqueous phase and interfacial material, which is predominantly laminin. Rotary evaporation was then used to reduce the volume of organic solvent. Renaturation of the receptor was achieved through exchange of the urea by the following series of dialysis steps: three changes of 1 M urea in methanol, three changes of 89% water, 10% methanol, 1% NP-40 in Dulbeco's phosphate buffered saline (DPBS), and four changes of 95% methanol. Dialysis into methanol was necessary to reduce the detergent concentration. The presence of detergent in the isolated material disrupted NMR spectroscopy of the peptides in the presence of receptor. The solution was then frozen at -70°C , lyophilized to dryness, and stored at -20°C .

Silver stained SDS-Page with a 5% to 15% acrylamide gradient of the final material revealed a single band at 67 kDa with a negligible amount of non-specific background (Fig. 3). In the gel presented in figure 3, lane A contained the molecular weight standards, lanes B and D contained material that had been reduced and lanes C and E contained unreduced material. The lower intensity of lanes B and D resulted from the lower concentrations of material found in the reduced solutions. The material extracted from tumor was reduced by heating for one hour at 80°C in a solution that was 20% glycerol, 2% sodium dodecyl sulfate (SDS), 2% beta-mercapto ethanol, and 0.05 M Tris-HCl, pH 8.6. The white powder produced by the extraction process, was used in TRNOESY NMR experiments without further purification.

Figure 3. SDS-Page of the Material Extracted From EHS Tumor.

The molecular weights (kDa) of the standard in lane A are given. The material in lanes B and D was reduced. Non-denatured material was run in lanes C and E.



Composition of Solution State NMR Samples

NMR spectroscopy of peptide 11, the d-analog, and the l-analog free in solution was performed on two sets of samples. The peptide concentration in both sets of NMR sample was approximately 10 mM. The first set of peptide 11, d-analog, and l-analog samples was dissolved in 90% H₂O/10% D₂O, 100 mM NaCl, 10 mM KPO₄, and 5 mM MgCl₂. Sodium azide at 0.02% was included as a bactericide. The pH of these solutions was in the range of 4.5 to 5, not correcting for isotope effects. The second set of peptide samples was dissolved in 90% Dulbecco's phosphate buffered saline (DPBS), which is 150 mM NaCl, 2.5 mM KCl, 1 mM CaCl₂, 0.5 mM MgCl₂ · 6 H₂O, 6.5 mM Na₂HPO₄ · 2 H₂O, 1.5 mM KH₂PO₄, and 10% D₂O. The pH of these samples was in the range of 7 to 7.6. The chemical shift standard employed was 3-(trimethylsilyl) propionic acid-2,2,3,3-d₄ (TSS).

NMR spectroscopy of peptides in the presence of the 67 kDa high-affinity laminin receptor was performed on samples which were ~1 mM in peptide and ~0.04 mM in receptor. The 67 kDa high-affinity laminin receptor has limited solubility in aqueous solution, and 3 mg per ml was the maximum attainable receptor concentration. As the receptor has a molecular weight of 67 kDa, it was assumed that the receptor was essentially pure and therefore the concentration was approximately 0.04 mM. Peptide 11 in the presence of receptor were made using both of the solutions used to study the peptides free in solution. The pH of these solutions was 5.0 and 7.6 respectively. Solutions of the d and l-analogs in the presence of receptor were made solely with DPBS. The pH of these solutions was 7.6 as well. DPBS was employed to study peptide in the presence of the receptor, because the 67 kDa

high-affinity laminin receptor appears to be more stable in aqueous solution in the presence of the divalent cations Ca^{2+} and Mg^{2+} (Jean Starkey and Terry Landowski, unpublished data).

The ratio of peptide to receptor in the NMR samples yields a $p_B \leq 2.5\%$. Although this p_B is relatively small, the TRNOESY cross peaks would be expected to be dominated by the bound form of the peptide due to the long τ_c expected for the 67 kDa high-affinity laminin receptor (Campbell and Sykes, 1991a). A low p_B produces the beneficial effect of reducing spin diffusion. As a result, the inter-proton distances of peptide 11, and the d and l-analogs derived from TRNOE peak intensities may reasonably be employed to calculate the receptor-bound peptide conformations; provided that the mixing times used are "reasonable" (Campbell and Sykes, 1991a).

NMR Spectroscopy Experimental Parameters

All NMR experiments were acquired at 500 MHz on a Bruker AM 500 with a 5 mm proton selective probe. The temperature of the sample was maintained at 274 K by a Eurotherm temperature control unit. Performing NMR spectroscopy of short, linear peptides in aqueous solution at low temperatures retards the exchange of amide protons, and increases the correlation time of the free peptide (Campbell and Sykes, 1991a). All spectra were acquired over a spectral width of 5263.16 Hz with the carrier frequency centered on the H_2O resonance. All spectra consisted of 512 t1 experiments, each with 2048 data points. 64 scans were time averaged per t1 experiment. Quadrature detection in t1 was achieved using time-proportional phase incrementation (TPPI) (Bodenhausen *et al.*, 1980, Marion and Wüthrich,

1983). At the experimental conditions described above, the longitudinal relaxation times (T_1) for the protons in the peptides ranged from 300 to 550 ms (Table 1). As an effective relaxation delay is 1 to 5 $\cdot T_1$, 1 second relaxation delay was deemed sufficient.

Table 1. Longitudinal Relaxation Times (T_1) of the Different Species of Protons Found in Peptide 11.

| Proton | T_1 (ms) |
|-----------------|------------|
| CH ₃ | 300 |
| CH ₂ | 300 |
| CH | 450 |
| aromatic | 550 |
| NH | 350 |

Total Correlation Spectroscopy (TOCSY) (Bax and Davis, 1985b, Bax, 1989, Cavanagh and Rance, 1990) incorporating the MLEV-17 spin lock sequence at a field strength of 10 kHz, and Rotating frame nuclear Overhauser Effect Spectroscopy (ROESY) (Bothner-By *et al.*, 1984, Bax and Davis, 1985a, Neuhaus and Keeler, 1986) utilizing a spin lock of 2.5 kHz for 200 ms, were utilized to assign the spectra. In these experiments the water resonance was suppressed by low power irradiation coherent with the transmitter phase during the relaxation delay.

Nuclear Overhauser Effect Spectroscopy (NOESY) (Jeener *et al.*, 1979) and transferred Nuclear Overhauser Effect Spectroscopy (TRNOESY) (Clare and Gronenborn, 1983, Campbell and Sykes, 1991a, Campbell and Sykes, 1991b) experiments were performed to estimate inter-proton distances. Water suppression in these experiments was obtained by Jump and Return (J+R)

detection (Plateau and Gueron, 1982). The pulse sequence of J+R NOESY experiments is presented in figure 4. By adjusting the receiver phase and incorporating a suitable delay immediately prior to signal detection it is possible to generate 2D J+R NOESY experiments that are in phase. Phasing with instrumental parameters is known as hardware phasing, a technique which greatly improved the ability to detect NOESY peaks in the resulting spectra by noticeably flattening the baseline. When processing the spectra only minor software phase corrections were necessary.

Processing of NMR Data

2D NMR data sets were processed on a Silicon Graphics 4D25TG workstation using the NMR processing software package, FELIX version 2.05 (© Hare Research Inc.). The 2 K by 0.5 K experimental data sets were converted to 1 K by 1 K matrices by deleting the imaginary points from the f2 dimension and zero filling the t1 dimension. Prior to Fourier transforming

Figure 4. J+R NOESY Pulse Sequence and Phase Cycling.

Pulse Sequence

D - 90°(PH1) - t1 - 90°(PH2) - t_m - 90°(PH3) - t₁ - 90°(PH4) - t₂ - t2(PH5)

Delays

D = 1 sec. relaxation delay
 t1 = 2D evolution period
 t_m = mixing time
 t₁ = 170 μsec. J+R delay
 t₂ = aquisition.
 t2 = first order phase delay

Phase Cycles

PH1 = 0 0 2 2 0 0 2 2
 PH2 = (8) 5
 PH3 = 0 1 0 1 2 3 2 3
 PH4 = 2 3 2 3 0 1 0 1
 PH5 = 0 1 2 3 0 1 2 3

(FT) t1 experiments (FIDs), a sine bell convolution difference (K=24) was applied at the carrier frequency to reduce residual water signals (Marion *et al.*, 1989). FIDs were also multiplied by a $\pi/6$ shifted sine bell window function in t2 to enhance resolution and an unshifted sine bell window function in t1. After transformation and phasing in the t2 dimension, a fifth order polynomial baseline correction algorithm was applied in f2. The data from experiments with jump and return detection were corrected for peak intensity distortion in f2 using a reciprocal sine correction function before transformation in the t1 dimension (Dratz and Lambert, unpublished).

Determination of Average Inter-Proton Distances

NOE and TRNOE intensities were converted into inter-proton distances so that experimentally estimated $\langle r_{ij} \rangle$ could be used to constrain molecular dynamics simulations. The average inter-proton distances of the compact conformations of peptide 11, the d-analog, and the l-analog free in solution were estimated from NOESY spectra with a t_m of 400 ms. NOESY cross peak volumes were measured using the NMR processing software, FELIX version 2.05 (© Hare Research, Inc., 1990).

Average inter-proton distances were then calculated according to the NOE intensity $r_{ij}^{-1/6}$ distance dependence using the $P_3\beta H^1-P_3\beta H^2$ NOE intensity and the known 1.89 Å inter-proton distance as a reference.

$r_{ij} = 1.89 \text{ \AA} \cdot (\text{NOE}_{P_3\beta H^1-P_3\beta H^2} / \text{NOE}_{ij})^{1/6}$ The NOE between the geminal β protons of proline was isolated in the NOESY spectra of peptide 11, the d-analog, and the l-analog and its intensity was readily measured. Using the $P_3\beta H^1-P_3\beta H^2$ NOE as a reference successfully predicted other known inter-

proton distances, such as the distance (1.76 Å) between the geminal γ protons of isoleucine ($I_6\gamma H_2^1-I_6\gamma H_2^2$). The inter-proton distances from sequential inter-residue NOE intensities (ie. $X_i\alpha H-Y_{i+1}NH$ and $X_i\beta H-Y_{i+1}NH$) were consistently predicted to be within their allowed ranges.

As has been discussed previously, the NOEs measured from a short peptide free in aqueous solution are indicative only of r_{ij} averaged largely over the most compact conformations of the peptide. In addition, intra-residue spin diffusion could have reduced the $P_3\beta H^1-P_3\beta H^2$ NOE intensity, which would result in the calculated distances being too short. Therefore, the $\langle r_{ij} \rangle$ calculated from the equation presented earlier should not be considered a precise measurement. In order to provide flexibility to the predicted inter-proton distances, after a distance was measured it was assigned to a 0.5 Å range. For example, if the $\langle r_{ij} \rangle$ was measured to be 2.65 Å, then r_{ij} was assigned to the range: $2.5 \text{ \AA} \leq r_{ij} \leq 3.0 \text{ \AA}$. The shortest range used was 1.5 Å - 2.0 Å and the longest was 3.5 Å - 4.0 Å. The longest range employed was 3.5 Å - 4.0 Å, because it is difficult to detect NOEs between protons which are greater than 3.5 Å apart in short, linear peptides free in aqueous solution (Wright *et al.*, 1988).

The method by which TRNOESY cross peaks were converted into inter-proton distances was quite different than the method used for free in solution NOE intensities. TRNOESY experiments were performed with 50 ms, 100 ms, 200 ms, and 400 ms mixing times. The range of inter-proton distance assigned to two protons was based on the length of the mixing time required for the cross peak to be detectable. If a NOE was first detectable using a 50, 100, or 200 ms mixing time, then r_{ij} was assigned to the range 2.0 - 2.5 Å,

